Protein folding stability and dynamics imaged in a living cell

Simon Ebbinghaus[1], Apratim Dhar[1], J Douglas McDonald[1] & Martin Gruebele[1–3]

Biomolecular dynamics and stability are predominantly investigated *in vitro* and extrapolated to explain function in the living cell. We present fast relaxation imaging (FreI), which combines fluorescence microscopy and temperature jumps to probe biomolecular dynamics and stability inside a single living cell with high spatiotemporal resolution. We demonstrated the method by measuring the reversible fast folding kinetics as well as folding thermodynamics of a fluorescence resonance energy transfer (FRET) probe-labeled phosphoglycerate kinase construct in two human cell lines. Comparison with *in vitro* experiments at 23–49 °C showed that the cell environment influences protein stability and folding rate. FReI should also be applicable to the study of protein-protein interactions and heat-shock responses as well as to comparative studies of cell populations or whole organisms.

Energy landscapes explain the dynamics of biomolecules *in vitro* and are usually considered a property of the individual biomolecule[1]. In the living cell, the biomolecular energy landscape is modulated by myriad interactions. The dynamics and stability of a protein crowded by up to 400 mg of macromolecules per milliliter of cytosol can differ substantially from the dynamics of the isolated protein[2,3]. Furthermore, crowding modifies the properties of cellular water, which can couple back to influence the dynamics of biomolecules[4]. Membranes and other large-scale structures in the cell can also crowd or confine biomolecules, as can the active interaction with cellular transport machinery or chaperones[5,6].

To reveal the full functionality of proteins and other biomolecules, they must be studied in the living cell. Several 'in cell' methods have emerged within the last two decades, yielding different types of information. Coherent anti-Stokes Raman scattering microscopy reports on small-molecule distributions inside living cells[7]. FlAsH dye–labeling can reveal slow urea-induced unfolding of proteins in bacterial cells[8]. Fluorescence resonance energy transfer (FRET) coupled with fluorescence microscopy can be used to localize proteins as well as monitor protein-protein interactions and the motion of larger protein machinery[9]. Fluorescent tracers used in fluorescence recovery after photobleaching or fluorescence correlation spectroscopy experiments can be used to monitor diffusion processes on a micrometer length scale[10,11]. NMR spectroscopy can reveal much detailed information about protein structure and dynamics inside living cells, but unlike the previous 'single-cell' techniques, NMR spectroscopy requires multiple cells to take up isotope-enriched proteins to enable detection of the desired protein. In-cell NMR spectroscopy experiments have been successful in yeast[12], bacteria (*Escherichia coli*)[13] and mammalian cells[14].

Here we introduce a technique that can be used to image the fast dynamics of biomolecules *in vivo* with subcellular resolution. Fast relaxation imaging (FReI) couples time-resolved fluorescence imaging with fast temperature jump–induced kinetics[15]. As a demonstration, we investigated unfolding and refolding of the metabolic enzyme phosphoglycerate kinase (PGK). We used a FRET probe–labeled fusion construct of PGK that unfolded at 39 °C in U2OS (human osteosarcoma) and HeLa (cervical carcinoma) cells. We also monitored the same construct *in vitro*. The protein was more stable, the thermal denaturation was more gradual, and folding kinetics were slower in our test cells than *in vitro*. Because biomolecular interactions are often highly temperature-sensitive, our method could be used to image many fast processes that occur in living cells, such as early events during heat-shock response or protein-protein interactions.

RESULTS

FReI methodology

Our goal was to study protein folding in a single cell, using a method whose time resolution is limited only by the induction time of the kinetics and whose spatial resolution is diffraction-limited. Our FreI method combines fluorescence microscopy of a FRET probe–labeled protein with small mid-infrared laser-induced temperature jumps. Temperature jumps cover a wide range of time scales. They equilibrate in aqueous medium within 2 ps[16], and have been carried out with picosecond lasers, nanosecond lasers as well as slower microwave and resistive heating techniques[15]. Imaging two-color fluorescence from a protein labeled with a donor-acceptor pair for FRET detection allowed us to interrogate the folding status of the construct in a cell by measuring the time evolution of the FRET signal after the temperature jump. We achieved reversible unfolding and refolding

[1]Department of Chemistry, [2]Department of Physics and [3]Center for Biophysics and Computational Biology, University of Illinois, Urbana, Illinois, USA. Correspondence should be addressed to M.G. (gruebele@scs.uiuc.edu).

RECEIVED 5 AUGUST 2009; ACCEPTED 29 DECEMBER 2009; PUBLISHED ONLINE 28 FEBRUARY 2010; DOI:10.1038/NMETH.1435

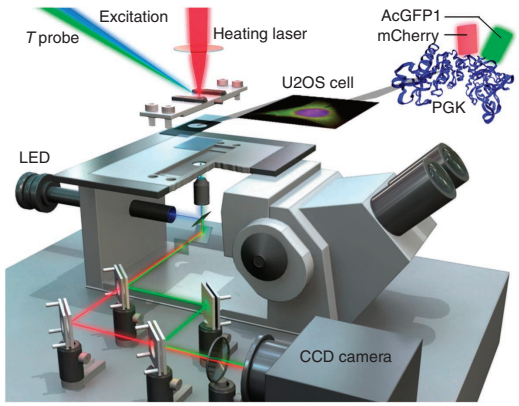

Figure 1 | Schematic of the temperature-jump fluorescence imaging microscope. The cells in the imaging chamber are illuminated by the blue LED or the argon ion laser to excite the FRET donor. The green laser probes the temperature (T probe) inside the cell by exciting the acceptor directly. A heating (infrared) laser initiates the temperature jump. The two-color fluorescent images are projected onto a CCD camera capable of recording millisecond time resolution movies of kinetics in the cell.

as well as temperature titrations across the unfolding transition of the labeled protein while the cell remained alive, as evidenced by cell morphology[17].

The upper temperature limit in our experiments was dictated by the temperature tolerance of the living cell. In general, the cell lines used must be sufficiently robust to tolerate small (≤4 °C) temperature jumps, exposure to mid-infrared light ($\lambda \approx 2{,}000$ nm) as well as visible-light probing FRET. This should be tolerated by many standard cell lines, such as the U2OS and HeLa lines used here, but will need to be checked carefully for more sensitive cells, such as mammalian neurons.

We transfected cells with plasmids encoding the FRET probe–labeled protein. We used green donor and red acceptor proteins with high melting points (>70 °C) as labels. Other colors or labeling techniques, such as dye labeling followed by microinjection, should be possible. Cells containing the FRET probe–labeled protein were adhered to a slide on a temperature-controlled stage during the experiment. The temperature-controlled stage was placed on an inverted fluorescence microscope (**Fig. 1**).

Two strategies can be used to excite the FRET donor: either a high-power blue light-emitting diode (LED) or a 458 nm argon ion laser line. The LED epi-illuminates the sample through an aspheric lens, beam-combining filters and the main microscope objective. The argon ion laser should be used for experiments that require high excitation intensities (low protein expression). Using an argon ion laser in epi-illumination leads to a speckled image, so this approach has been used only for confocal or single-molecule particle-tracking experiments[18,19] not for full cell imaging. Somewhat involved schemes have been proposed to reduce coherence speckles during full imaging[20,21]. We solved this problem by focusing the laser onto the sample in a highly oblique trans-illumination mode with a long focal length (50 cm) lens (**Fig. 1**). This increased the speckle size to the size of the field, uniformly illuminating the sample.

We collected red and green fluorescence through the objective and beam combining filters, and then split the signal into a red and a green channel, which we imaged onto adjacent spots of a single charge-coupled device (CCD) sensor. Our camera recorded a frame every 16.7 ms. The frame rate, not the temperature-jump rate, currently limits the time resolution of the experiment and could easily be sped up by using commercially available cameras with microsecond time resolution.

To study kinetics, a computer-tailored infrared diode laser initiated fast upward and downward laser temperature jumps in the cell and its surrounding aqueous medium. The 2,200 nm infrared wavelength is absorbed uniformly by water inside and outside the cell, causing a step-shaped temperature rise within the acquisition time of the camera. We used two types of pulses. To achieve a fast upward jump only, we shaped the laser power into a spike followed by a plateau to raise the temperature rapidly, then keep it constant (**Fig. 2a**). To achieve a fast (<50 ms) downward jump, we used the laser to preheat the cell to a constant temperature, spiked and plateaued the power, then dropped to zero laser power to accelerate cooling, and finally raised laser power to the preheating level to yield a box-shaped heating profile (**Fig. 2a**).

We monitored the temperature profile pixel by pixel *in vitro* or directly in the cell by exciting the acceptor label with a green diode laser (**Fig. 2b**). We calibrated the acceptor fluorescence intensity to an absolute temperature scale with a thermocouple mounted on the stage or on the slide below the cell. With our setup, the temperature was uniform to single-pixel resolution, although implementation of temperature gradients across the cell to induce differential stress may be of interest in future applications.

For small jumps, the protein unfolding and refolding kinetics were completely reversible and returned to the same donor to acceptor FRET ratio (D/A) baseline in the cell (**Fig. 2c**). The initial very fast rise of D/A was due to a combination of an intrinsic fluorescence baseline (**Fig. 3a** and Online Methods), and a small sub-millisecond kinetic burst phase, resolved in previous *in vitro* studies[22]. The subsequent time-resolved increase of D/A resulted from unfolding of the protein construct (see below). At least for U2OS and HeLa cells studied here, irreversible effects caused by aggregation or heat-shock response were observed only for much

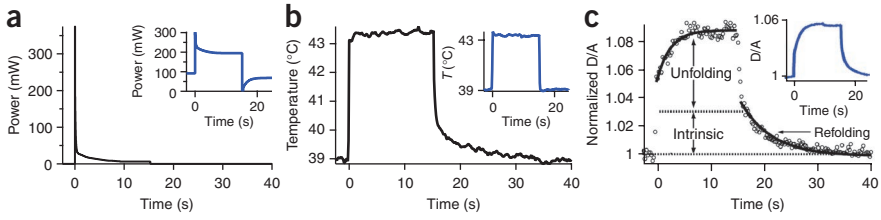

Figure 2 | Heating laser profiles, resulting temperature profiles and folding kinetics of the low-T_m PGK construct. (**a**) Laser profiles for a fast upward temperature jump of 4 °C and for a <50 ms downward jump (inset). (**b**) Corresponding temperature profiles measured directly in a U2OS cell and *in vitro* (inset) by mCherry fluorescence. (**c**) Protein unfolding (t = 0–15 s) and refolding (t = 15–40 s) in a U2OS cell and *in vitro* (inset). The initial fast rise contains an unresolved burst phase and an intrinsic fluorescence baseline (see **Fig. 3a**). The subsequent resolved phase monitors unfolding of the PGK fusion construct. After the temperature jump is switched off, the protein refolds to the original baseline, indicating complete reversibility both in the cell and *in vitro*.

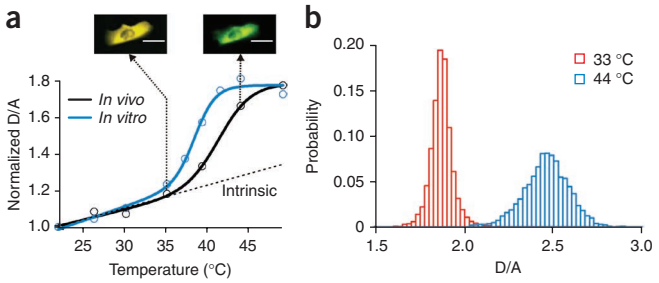

Figure 3 | Temperature-dependent FRET and thermal denaturation of the low-T_m PGK fusion construct. (**a**) Sigmoid fit to the *in vivo* D/A upon thermal denaturation (*in vivo*) compared to *in vitro*. The dotted line shows the intrinsic native state fluorescence baseline, which causes a small part of the instantaneous kinetic response (see **Fig. 2c**). Fluorescence images of the U2OS cell at the temperatures indicated by the arrows are shown. Scale bars, 20 μm. (**b**) FRET D/A distributions at the indicated temperatures.

larger temperature jumps and much longer heating times than the 15 s, 4 °C temperature step we used. Slow infrared heating up to 60 °C has been used to study heat-shock response and gene induction *in vivo*[23].

In a typical FreI experiment, the cell was gradually heated on the stage, and a heat-denaturation curve of the protein was recorded as D/A within a few minutes. At each steady-state temperature, a small temperature jump (typically 4 °C) then was used to measure the relaxation kinetics. To account for inactive acceptor labels, the data were referenced to a low temperature (23 °C) where most protein was folded (Online Methods). Thus stability and kinetic data can be collected in the same experiment on one cell. Notably, denaturation transitions and lifetime measurements were insensitive to absolute fluorescence variations across the cell caused by different cell thicknesses, for example.

PGK unfolding *in vivo*

To assess the performance of FReI, we studied PGK unfolding in easily cultured U2OS cells (**Figs. 2–4**). We wanted to understand how kinetics of unfolding in cells differed from *in vitro* conditions, using the same instrument to make our measurements. With a properly tailored heating and cooling pulse (**Fig. 2b**), a similar analysis could also be carried out for refolding, albeit with lower time resolution (**Fig. 2c**).

PGK was the protein of choice for our initial studies because previous *in vitro* experiments revealed stretched exponential kinetic phases ranging from microseconds to minutes[22,24]. Thus, we expected substantial unfolding within the experimental time window (16 ms to 15 s) studied here. We designed a fusion protein consisting of mutant PGK labeled on its N and C termini by AcGFP1 (green donor) and mCherry (red acceptor), respectively. We used a low-melting-temperature triple mutant (Y122W,W308F,W333F) of PGK[22]. This construct allowed us to study unfolding titrations and kinetics at near-physiological temperatures that are not harmful to the U2OS cells and that avoid the heat-shock response. A high-melting-temperature double mutant (W308F,W333F; melting temperature, $T_m > 45$ °C) was used as a reference that would not unfold below 45 °C. The fluorescent labels did not unfold up to 70 °C *in vitro* (cell death is the *in vivo* upper temperature limit). Cell morphology served as an indicator of viability in all experiments[17], and temperatures up to 49 °C could be reached in these cells.

To measure protein stability in the cell and monitor folding, we measured the D/A of the PGK fusion protein construct as a function of temperature, relative to the D/A at 23 °C. The D/A yielded a sigmoidal unfolding curve *in vitro* and *in vivo* (**Fig. 3a**). Unfolding was more gradual and stability was slightly greater in the cell; T_m of the protein in cells was 42 °C versus 39 °C in solution. We thus expected that temperature jumps starting at 39 °C should lead to observable kinetics, and temperature jumps in the baselines (below 30 °C or above 45 °C) would yield only a small instantaneous response of the completely folded or completely unfolded protein. The FRET ratio showed the expected broadening and shift caused by unfolding through several intermediates at higher temperature; as the protein unfolded the N and C termini moved further away from each other, leading to a decrease in FRET (**Fig. 3b**). The signal–to-noise ratio shown (**Figs. 3** and **4**) required a protein column density of about 1,000 μm^{-2} in the cell (Online Methods).

We investigated the low-melting-temperature PGK mutant unfolding kinetics (and refolding kinetics; **Fig. 2c**) starting at different initial temperatures but with the same temperature-jump magnitude of 4 °C. We observed very different responses at 27 °C, 39 °C and at 49 °C (**Fig. 4**). As expected from the thermodynamic measurements, jumping from an initial temperature of 27 °C yielded no response because no protein unfolding occurred. With temperature jumps from 39 °C by +4 °C, we resolved a large change in the D/A as the protein thermally unfolded. The unfolding signal was well described by a signal function $S(t) = A \exp(-(t/\tau)^{\beta})$, yielding a time constant of $\tau = 3.01 \pm 0.04$ s. (The stretching factor β allowed a simplified fit to multi-intermediate kinetics and yielded values in the range 0.67–0.87 in all cases.) Jumping from 49 °C yielded only a small fast decrease in D/A after the jump. This was due to a small amount of aggregation at high temperature, which causes intermolecular FRET and therefore a decrease of D/A. The high-melting-temperature PGK mutant had no kinetic phase at 39 °C, as expected (**Fig. 4b**).

We repeated the same temperature-jump experiments with the low-melting-temperature PGK construct in aqueous solution at

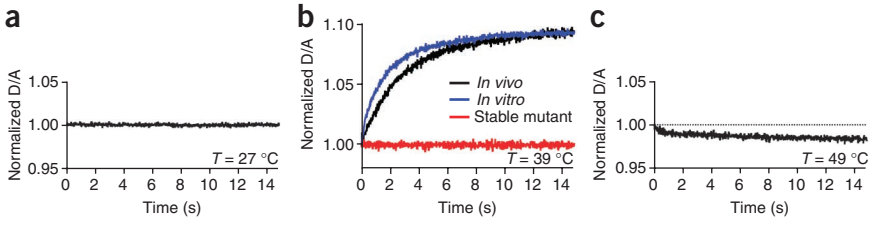

Figure 4 | Normalized D/A relaxation kinetics of the PGK fusion protein *in vivo* and *in vitro* track the denaturation curves. (**a**) Normalized D/A after a temperature jump from 27 to 31 °C on the folded state baseline (dotted line labeled "intrinsic" in **Fig. 3a**) showed no unfolding of the less stable PGK after the jump. (**b**) Normalized D/A after a temperature jump from 39 to 43 °C, near the melting temperature, resolves unfolding of the less stable construct *in vitro* and *in vivo* but not for the more stable mutant. (**c**) Normalized D/A after a temperature jump from 49 to 53 °C on the unfolded baseline, showing no additional unfolding of the less stable protein. Instead a small decrease of the D/A was observed, presumably owing to aggregation and intermolecular FRET.

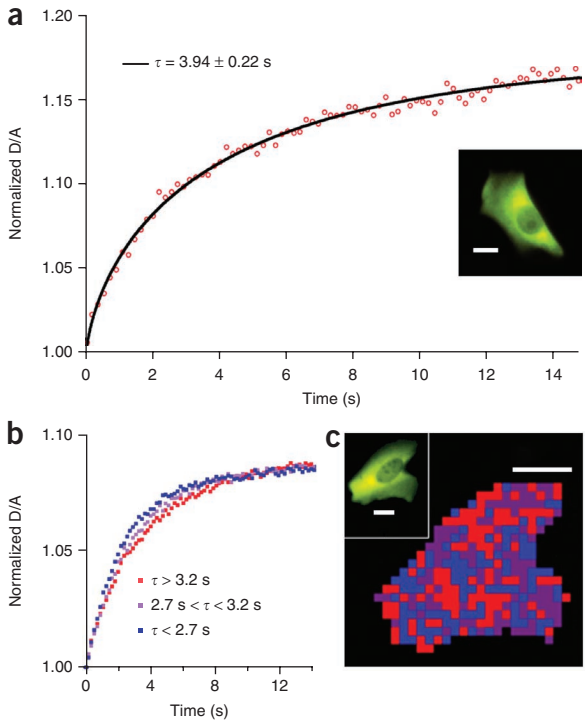

Figure 5 | Comparison of folding kinetics of the less stable PGK mutant in two cell lines. (**a**) Folding relaxation trace averaged over a HeLa cell for a temperature jump from 39 to 43 °C. Inset, fluorescence image of the HeLa cell. (**b**) Spatially resolved folding relaxation traces in a U2OS cell, distinguishing zones of fast (<2.7 s), medium (2.7–3.2 s) and slow (>3.2 s) folding. (**c**) Color-coded image for the three zones in **b**. Inset, fluorescence image of the U2OS cell. Scale bars, 10 μm.

pH 7 and observed faster kinetics. After a jump from 39 °C (**Fig. 4**), we observed a relaxation time of $\tau = 1.95 \pm 0.22$ s. Thus the environment in the cytoplasm of this particular cell slowed down the unfolding kinetics.

We repeated the *in vivo* experiment in HeLa cells to determine whether different cell lines can be used in our experiment; in the HeLa cell, the kinetics were slowed down even more ($\tau = 3.94 \pm 0.22$ s) compared to the *in vitro* value (**Fig. 5a**). Finally, we imaged the U2OS cell and could distinguish cytoplasmic regions of short (<2.7 s), medium (2.7 to 3.2 s) and long (>3.2 s) unfolding times within the same cell. The largest homogenous regions were ~8 μm in diameter (**Fig. 5b**,**c**). This could be due to PGK associating with membranes or other subcellular structures.

DISCUSSION

The fusion protein studied here closely resembles hisPGK122, which has been studied *in vitro* by refolding from the cold denatured state[22]. The measured folding relaxation times for hisPGK122 range from microseconds to seconds, which explains the observation of a burst phase in addition to the resolved kinetics we observed for our low-melting PKG construct[22,24].

Our method allows us to compare the behavior of the same protein construct inside a single living cell directly with dilute solution. The increased T_m we observed *in vivo* in both cell types could be due to the cytoplasm having a high concentration of macromolecules. A crowded environment can enhance the native state stability relative to the unfolded state by restricting the conformational freedom of the latter[2]. Folding was slower in both cells studied here than *in vitro*, indicating higher viscosity or higher activation energy within the cell. Moreover, the activation energy or viscosity (or both) were position-dependent within the cell. The observed folding time τ could be slowed down or sped up, depending on whether increased viscosity of the cytoplasm or reduced unfolded state entropy dominates. Indeed, models predict a non-monotonic dependence of the rate of folding on the crowding fraction[2].

Although we so far have only tested the method with a single protein in two cell lines, and over a limited temperature range (23–49 °C), our results point to interesting questions. What would a high-resolution spatial map of protein stability in a single cell look like? The observed low cooperativity in the cell could be due to averaging over different protein stabilities in different parts of the cell, or it could be truly lower cooperativity of individual protein molecules. Different expression levels coupled with diffraction-limited resolution of the thermodynamics could be used to probe the extent to which the cytoplasm modulates protein stability[25]. Detailed comparison among different cells from the same cell line and among different cell lines will also be of interest for addressing the question of whether protein stability and folding rate vary more within a single cell than among different cells.

Processes besides folding can be observed by FReI, and for such processes physiological temperature limits are less of an experimental hindrance. Tracking cell-specific protein dynamics in entire cell populations will help us understand processes such as stochastic gene expression[26], cell division[27] or apoptosis[28]. Rapid temperature-sensitive protein-protein interactions or aggregate formation in cells could be perturbed and monitored as they relax back toward steady state. For example, chaperone binding upon heat-shock response could slow the refolding relaxation rate relative to the unfolding relaxation rate. Finally, *in vivo* kinetic assays could be developed in organisms amenable to microscopy studies. For example, temperature-sensitive small-molecule binding is useful for drug screening or searching for compounds that act as protein misfolding medication[29], and fundamental processes such as the heat-shock response could be studied *in vivo*.

METHODS

Methods and any associated references are available in the online version of the paper at http://www.nature.com/naturemethods/.

ACKNOWLEDGMENTS

We acknowledge funding from the US National Science Foundation (MCB 0613643). A.D. was supported by the National Science Foundation Center for Physics of Living Cells (Illinois Physics Department) while part of this work was carried out. S.E. and M.G. acknowledge support from the Alexander von Humboldt Foundation. We thank Z. Shen and K.V. Prasanth for growing the U2OS and HeLa cell lines.

AUTHOR CONTRIBUTIONS

A.D. and S.E. designed and implemented instrumentation and software, performed experiments, analyzed data and wrote the paper. J.D.M. designed experimental components. M.G. designed the experiment, analyzed data and wrote the paper.

COMPETING FINANCIAL INTERESTS

The authors declare no competing financial interests.

Published online at http://www.nature.com/naturemethods/.
Reprints and permissions information is available online at http://npg.nature.com/reprintsandpermissions/.

1. Frauenfelder, H., Sligar, S.G. & Wolynes, P.G. The energy landscapes and motions of proteins. *Science* **254**, 1598–1603 (1991).
2. Cheung, M.S., Klimov, D. & Thirumalai, D. Molecular crowding enhances native state stability and refolding rates of globular proteins. *Proc. Natl. Acad. Sci. USA* **102**, 4753–4758 (2005).
3. Ignatova, Z. *et al.* From the test tube to the cell: exploring the folding and aggregation of a beta-clam protein. *Biopolymers* **88**, 157–163 (2007).
4. Frauenfelder, H., Fenimore, P.W., Chen, G. & McMahon, B.H. Protein folding is slaved to solvent motions. *Proc. Natl. Acad. Sci. USA* **103**, 15469–15472 (2006).
5. Johnson, J.L. & Craig, E.A. Protein folding *in vivo*: unraveling complex pathways. *Cell* **90**, 201–204 (1997).
6. Hartl, F.U. & Hayer-Hartl, M. Converging concepts of protein folding *in vitro* and *in vivo*. *Nat. Struct. Mol. Biol.* **16**, 574–581 (2009).
7. Evans, C.L. & Xie, X.S. Coherent anti-Stokes Raman scattering microscopy: chemical imaging for biology and medicine. *Annu. Rev. Anal. Chem.* **1**, 883–909 (2008).
8. Ignatova, Z. & Gierasch, L.M. Monitoring protein stability and aggregation *in vivo* by real-time fluorescent labeling. *Proc. Natl. Acad. Sci. USA* **101**, 523–528 (2004).
9. Kural, C. *et al.* Kinesin and dynein move a peroxisome *in vivo*: a tug-of-war or coordinated movement? *Science* **308**, 1469–1472 (2005).
10. Luby-Phelps, K., Castle, P.E., Taylor, D.L. & Lanni, F. Hindered diffusion of inert tracer particles in the cytoplasm of mouse 3t3 cells. *Proc. Natl. Acad. Sci. USA* **84**, 4910–4913 (1987).
11. Lippincott-Schwartz, J., Snapp, E. & Kenworthy, A. Studying protein dynamics in living cells. *Nat. Rev. Mol. Cell Biol.* **2**, 444–456 (2001).
12. Williams, S.P., Haggie, P.M. & Brindle, K.M. F-19 NMR measurements of the rotational mobility of proteins *in vivo*. *Biophys. J.* **72**, 490–498 (1997).
13. Serber, Z. *et al.* High-resolution macromolecular NMR spectroscopy inside living cells. *J. Am. Chem. Soc.* **123**, 2446–2447 (2001).
14. Inomata, K. *et al.* High-resolution multi-dimensional NMR spectroscopy of proteins in human cells. *Nature* **458**, 106–109 (2009).
15. Gruebele, M. Fast protein folding kinetics. in *Protein Folding, Misfolding and Aggregation* (ed. Muñoz, V.) 106–138 (RSC Publishing, London, 2008).
16. Ma, H.R., Wan, C.Z. & Zewail, A.H. Ultrafast T-jump in water: studies of conformation and reaction dynamics at the thermal limit. *J. Am. Chem. Soc.* **128**, 6338–6340 (2006).
17. Clarke, P.G.H. Developmental cell-death—morphological diversity and multiple mechanisms. *Anat. Embryol. (Berl.)* **181**, 195–213 (1990).
18. Yu, J., Xiao, J., Ren, X.J., Lao, K.Q. & Xie, X.S. Probing gene expression in live cells, one protein molecule at a time. *Science* **311**, 1600–1603 (2006).
19. Brandenburg, B. *et al.* Imaging poliovirus entry in live cells. *PLoS Biol.* **5**, 1543–1555 (2007).
20. Mattheyses, A.L., Shaw, K. & Axelrod, D. Effective elimination of laser interference fringing in fluorescence microscopy by spinning azimuthal incidence angle. *Microsc. Res. Tech.* **69**, 642–647 (2006).
21. Dingel, B. & Kawata, S. Speckle-free image in a laser-diode microscope by using the optical feedback effect. *Opt. Lett.* **18**, 549–551 (1993).
22. Osvath, S., Sabelko, J.J. & Gruebele, M. Tuning the heterogeneous early folding dynamics of phosphoglycerate kinase. *J. Mol. Biol.* **333**, 187–199 (2003).
23. Kamei, Y. *et al.* Infrared laser-mediated gene induction in targeted single cells *in vivo*. *Nat. Methods* **6**, 79–81 (2009).
24. Osvath, S., Herenyi, L., Zavodszky, P., Fidy, J. & Kohler, G. Hierarchic finite level energy landscape model to describe the refolding kinetics of phosphoglycerate kinase. *J. Biol. Chem.* **281**, 24375–24380 (2006).
25. Wibo, M. & Poole, B. Protein degradation in cultured cells. 2. Uptake of chloroquine by rat fibroblasts and inhibition of cellular protein degradation and cathepsin-B1. *J. Cell Biol.* **63**, 430–440 (1974).
26. Golding, I., Paulsson, J., Zawilski, S.M. & Cox, E.C. Real-time kinetics of gene activity in individual bacteria. *Cell* **123**, 1025–1036 (2005).
27. Kar, S., Baumann, W.T., Paul, M.R. & Tyson, J.J. Exploring the roles of noise in the eukaryotic cell cycle. *Proc. Natl. Acad. Sci. USA* **106**, 6471–6476 (2009).
28. Leadsham, J.E. & Gourlay, C.W. Cytoskeletal induced apoptosis in yeast. *Biochim. Biophys. Acta* **1783**, 1406–1412 (2008).
29. Vieira, M.N.N., Figueroa-Villar, J.D., Meirelles, M.N.L., Ferreira, S.T. & De Felice, F.G. Small molecule inhibitors of lysozyme amyloid aggregation. *Cell Biochem. Biophys.* **44**, 549–553 (2006).

ONLINE METHODS

Protein engineering. The plasmid for the phosphoglycerate kinase (PGK) fusion protein was created by ligating the genes for AcGFP1 (Clontech) and mCherry (Clontech) to the 5′ and 3′ ends, respectively, of the gene encoding the Y122W,W308F,W333F mutant of PGK. This gene was cloned into the pDream 2.1 vector (Genscript). This vector has both a T7 promoter for expression in *E. coli* and a CMV promoter for expression in mammalian cells. A 6His tag was added to the N terminus of AcGFP1 to enable purification on a Ni-NTA column (Qiagen) for *in vitro* studies. To obtain a protein stable at 39–43 °C, we also made the Y122W construct, which differs by only one tryptophan from wild type and is nearly 20 kJ mole^{-1} more stable based on guanidinium denaturation.

To obtain the fusion proteins for *in vitro* characterization, BL21-CodonPlus (DE3)-RIPL cells (Stratagene) were transformed with the plasmid and grown in Luria-Bertani medium to an optical density of 0.8, at which time protein expression was induced by addition of 1 mM IPTG (Inalco). After induction, cells were grown at 23 °C for 12 h, collected by centrifugation and lysed using a French press. Cell lysate was bound to a Ni-NTA column and purified according to the manufacturer's protocol. Purity of the protein was determined by SDS-PAGE and electrospray ionization mass spectrometry (ESI MS). For the *in vitro* experiments, we used a 10 μM solution of the PGK fusion protein, placed in an imaging chamber (construction described below), and studied it under the same experimental conditions as used for the *in vivo* experiments.

Cell culture. U2OS and HeLa cells were grown in 35 mm Petri dishes (Corning) in DMEM (Hyclone) supplemented with penicillin-streptomycin (PS) and 10% FBS to >70% confluency. Transient transfection was performed with Lipofectamine (Invitrogen) per the manufacturer's protocols. Six hours after transfection, cells were split and grown on coverslips. Cells were imaged 24–48 h after transfection. Immediately before imaging, cells were transferred into imaging chambers filled with Liebovitz L-15 medium (Gibco) supplemented with PS and 30% FBS. Imaging chambers were formed by putting together a coverslip with adherent cells onto a standard 1 × 3 inch microscope slide, separated by a 100 μm spacer (Grace Bio Labs).

Microscopy equipment and settings. Cells were imaged on an Axiovert 100TV inverted microscope (Zeiss). Imaging chambers (glass slides with 100 μm spacers) were mounted on a custom-designed brass and Delrin microscope stage and held in place by an aluminum cover plate to provide thermal stability and rapid thermal equilibration (**Fig. 1**). Steady-state heating was achieved with two thermistors mounted on the aluminum plate. A small hole was drilled in this plate to pass the argon ion laser and infrared heating beam through while minimizing exposed surface area of the slide and coverslip.

The cells were illuminated by a high power LED (Luxeon) or by the 458 nm line from an argon ion laser (Coherent). The LED was mounted on the back of the microscope and collimated using a home-built optical train consisting of a 50 mm aspheric lens and a 150 mm planoconvex lens (**Fig. 1**). The collimated beam was passed through the excitation filter (Chroma; ET470/40×) and focused by a 40× microscope objective (Zeiss) with numerical aperture of 0.65. The emitted two-color fluorescence (from AcGFP1 and mCherry) was collected by the same objective and separated from the blue excitation beam by a dichroic mirror (Chroma; T495LP) and a longpass emission filter (Omega; XF3108/25). The two-color fluorescence was separated into green and red components by using a second dichroic mirror (Chroma; T585LP) before being simultaneously imaged onto different positions on a charge-coupled device (CCD) camera (Lumenera Corporation) operating at 60 frames per second (**Fig. 1**). Typical signal levels corresponded to a column density of <1,000 proteins μm^{-2}, estimated by comparing cell signal levels with *in vitro* solutions of protein, with a correction for focal depth of the fluorescence collection.

When using the argon ion laser for illumination, a prism selected the 458 nm line. The beam was then passed through a narrow bandpass filter (Chroma; Z458/10×) to remove any stray light. The laser illuminated the sample from the top (in a trans-illumination configuration) rather than through the objective. We used a long focal length lens (f = 50 cm) to achieve speckle-free imaging with the laser source, by enlarging the speckles to greater than the size of a cell.

Videos of the cell under observation were recorded by custom-written software in Labview (National Instruments). The red and green fluorescence images, projected onto adjacent areas of the same CCD sensor were superimposed onto each other with single pixel accuracy. This was achieved by computing the cross-correlation function between the two images and translating as well as rotating one image to maximize the cross-correlation. The mean intensity of each image was calculated and plotted against the acquisition time for cell-averaged kinetics. Dividing the green by red intensity yielded the FRET signal (D/A). Because different cells have different ratios of intact fusion construct to constructs with mCherry improperly folded or bleached, all data were referenced to the D/A ratio at 23 °C (scaled value of 1 in **Figs. 2c**, **3a** and **4**). For comparison of *in vitro* to *in vivo* profiles, the former amplitude was also normalized to the latter. For images in **Figures 3a** and **5a**, red and green fluorescence images were overlaid using ImageJ (US National Institutes of Health) to obtain the pseudo-colored images. Pseudocolor was obtained by adding the original 8 bit values in the red (R) and green (G) fluorescence channels into an RGB color (R,G,0). The specific settings for the images in the main text were: **Figures 3a** and **5a**, resolution 0.43 μm per pixel, 16 ms integration time; and **Figure 5c**, binned resolution 1.3 μm pixel^{-1} (31 pixels horizontal).

Temperature sensing and calibration. The temperature was calibrated both from above (slide) and below (coverslip) the stage by thermocouples. A thermocouple also provided a feedback signal for the heating resistors to keep the temperature stable within ± 0.5 °C. To monitor the temperature in the living cell directly by mCherry fluorescence, a 532 nm diode laser (Casix) was used in the same configuration as the blue diode. The resulting red fluorescence was separated from the excitation light by a band-pass emission filter (Chroma; ET630/75m). The red fluorescence is temperature-sensitive, and was calibrated against the stage thermocouples. A final independent calibration of the temperature of the entire 100 μm sample height, also suitable for *in vitro* measurements, was provided by a 1,500 nm laser diode passed through the sample and chopped at 2 kHz for detection by an infrared detector (Infrared Associates MCT) coupled to a lock-in

doi:10.1038/nmeth.1435

amplifier (Stanford Research Associates). Water transmission at 1,500 nm is temperature-sensitive and was again calibrated against thermocouples. All these methods showed for *in vivo* and *in vitro* excitation that the temperature and temperature jumps were uniform to the single-pixel level of resolution.

Temperature jumps. Unfolding and refolding of the fusion protein was rapidly initiated by a large area tailored heating pulse from an infrared diode laser operating at 2,200 nm (m2k laser). The laser was mounted on a breadboard above the stage of the inverted microscope. We designed two laser output power profiles (**Fig. 2a**) by mapping out the instrument response function with a millisecond square pulse, followed by Fourier deconvolution of the desired response with the instrument response function. One profile (overshoot plus plateau) resulted in rapid heating followed by a constant temperature for an arbitrary amount of time. Picosecond jumps could be achieved in principle, although our laser electronics are limited to sub-millisecond time scales. A second profile achieved fairly rapid downward jumps with <50 ms time resolution by undershooting the laser power and then ramping it back up to provide an optimal downward step. Cooling of the thin aluminum-covered glass slides can be quite fast. An achromatic lens (f = 25 mm) was used to focus the laser beam to 500 μm in diameter, allowing uniform heating over 25 times the area of the cell being imaged. Temperature jump size was calibrated by monitoring mCherry fluorescence (*vide supra*).

Statistical data analysis. The stretched exponential relaxations were fitted in Mathematica (Wolfram Research) or Igor Pro (Wavemetrics) using a nonlinear least square fitting routine (Levenberg–Marquardt algorithm). The uncertainties reported are ± 2 s.d.